Food Chemistry: X 15 (2022) 100389

Contents lists available at ScienceDirect

Food Chemistry: X

journal homepage: www.sciencedirect.com/journal/food-chemistry-x

Interaction and binding mechanism of lipid oxidation products to sturgeon myofibrillar protein in low temperature vacuum heating conditions: Multispectroscopic and molecular docking approaches

Shi-ke Shen [a,b], Qian-yun Bu [a,b], Wen-tao Yu [a,b], Yue-wen Chen [a,b,*], Fei-jian Liu [a,b], Zhi-wen Ding [a,b], Jun-long Mao [a,b]

[a] School of Food Science and Biotechnology, Zhejiang Gongshang University, Hangzhou, Zhejiang 310035, People's Republic of China
[b] Zhejiang Provincial Collaborative Innovation Center of Food Safety and Nutrition, Zhejiang Gongshang University, Hangzhou, Zhejiang 310035, People's Republic of China

ARTICLE INFO

Keywords:
Sturgeon myofibrillar protein
Malondialdehyde
4-Hydroxy-2-nonenal
Molecular docking
Binding mechanism
Low temperature vacuum heating

ABSTRACT

In this work, the binding mechanism of myofibrillar protein (MP) with malondialdehyde and 4-hydroxy-2-nonenal under low temperature vacuum heating was investigated *via* multispectroscopic and molecular docking. The results showed that binding interaction and increasing temperature caused significant changes in the conformations as well as a decrease in the value of protein intrinsic fluorescence, surface hydrophobicity, and fluorescence excitation-emission matrix spectra. Furthermore, the decrease in α-helix and β-turn, increase in β-sheet and a random coil of MP, imply the MP molecules to be more unfolded. Isothermal titration calorimetry and molecular docking results showed that main driving force for binding with MP was hydrogen bond, and the binding ability of malondialdehyde was superior to that of 4-hydroxy-2-nonenal. Moreover, increasing the heating temperature was beneficial to the binding reaction and intensified the conformational transition of MP. These results will provide a reference for further studies on the lipid and protein interaction of sturgeon.

1. Introduction

Russian sturgeon (*Acipenser gueldenstaedti*), as a typical source of highly digestible protein, is increasingly farmed due to its rich protein and polyunsaturated fatty acids, as well as its balanced amino acid composition (Liu et al., 2022), especially in China, which accounts for 85% of global production (Shen et al., 2020). At present, the processing of sturgeon fillets is still relatively basic, and an important reason is a loss caused by protein oxidation during processing. Protein oxidation changes the physicochemical properties of the protein in sturgeon fillets, which in turn affects the quality of sturgeon fillets and their processing properties (Zhang, Xiao, & Ahn, 2013). Regulation of protein oxidation during processing is a critical issue for improving sturgeon utilization.

Heat treatment is a common technical unit in the prefabrication or cooking process of fish meat. Most of the traditional heat treatment methods are air exposure conditions under normal pressure. The oxidative structure of protein is relatively serious, and it is easy to cause quality deterioration and economic losses due to excessive heat processing (Wan et al., 2021). Low temperature vacuum heating (LTVH) is a new heating technique, which can effectively improve the processing quality of sturgeon meat, form a good flavor (Liu et al., 2022), and prolong the shelf life (Shen et al., 2020). Compared to other vacuum heat treatment methods, LTVH was an easy-to-use processing method for processing large batch sizes of samples simultaneously. Therefore, LTVH is more suitable for industrial production. Based on this, it is necessary to study protein oxidation under LTVH processing conditions to expand the production and utilization of sturgeon fillets.

Protein and lipid oxidation reactions usually co-exist and mutually promote one another in the meat system (Wang, Zhao, Qiu, & Sun, 2018). The oxidation of both was generally initiated by reactive oxygen species (ROS), and there was a potential correlation between the two (Wang, He, Emara, Gan, & Li, 2019). Lipid oxidation products can cause

Abbreviations: LTVH, low temperature vacuum heating; MDA, malondialdehyde; HNE, 4-hydroxy Nonenal; MP, myofibrillar protein; Trp, tryptophan; Tyr, tyrosine; ITC, isothermal titration calorimetry.

* Corresponding author at: School of Food Science and Biotechnology, Zhejiang Gongshang University, Xiasha University Town, Hangzhou, People's Republic of China.
E-mail address: chenyw@zjgsu.edu.cn (Y.-w. Chen).

https://doi.org/10.1016/j.fochx.2022.100389
Received 19 April 2022; Received in revised form 2 July 2022; Accepted 5 July 2022
Available online 8 July 2022

some damage to the protein. 4-Hydroxy-2-nonenal (HNE) altered the spatial structure of the protein and damaged the membrane of the protein, resulting in changes in membrane protein function, for example, Na^+/K^+ ion pump activity decreased (Fleuranceau-Morel, Barrier, Fauconneau, Piriou, & Huguet, 1999). Some studies have mainly focused on the oxidative damage of malondialdehyde (MDA) on myofibrillar protein (Wang et al., 2019) and the properties of myofibril gel (Wang, Zhang, Fang, & Bhandari, 2017), and some scholars have also paid attention to the effect of MDA on protein after adding antioxidants (Wang, He, Zhang, Chen, & Li, 2021). Previous studies did not apply external force and only relied on the interaction of MDA with proteins to promote protein oxidation. However, in the actual production process, factors such as heating, high pressure, and electric field will affect protein oxidation together with lipid oxidation products. Nevertheless, it is reasonable to speculate the LTVH could accelerate the reaction of lipid oxidation products and proteins, and the degree of both reactions increased with increasing temperature.

The purpose of this paper was to study the interaction and binding mechanism of different lipid oxidation products (MDA and HNE) on sturgeon myofibrillar proteins under low temperature vacuum heating (50, 60, 70 °C respectively). The multispectral methods including intrinsic fluorescence spectroscopy, Fourier transformation infrared (FTIR) spectroscopy, fluorescence excitation-emission matrix (EEM) spectra were used to analyze the structural changes in proteins. Meanwhile, the affinity of the interaction was confirmed by isothermal titration calorimetry (ITC). Besides, molecular docking technology was used to explore the binding mechanism of MDA and HNE to MP. The research results can provide new ideas for regulating protein oxidation during heating, and provide theoretical support for deep processing of sturgeon.

2. Materials and methods

2.1. Materials

The sturgeon was transported from Quzhou Sturgeon Aquatic Food Technology Development Co. Ltd. (Zhejiang, China) within 2 h at 4 °C. 4-hydroxy Nonenal (HNE) was purchased from GlpbBio (Shanghai, China), sodium phosphate Dibasic dodecahydrate, 1,1,3,3-Tetramethoxypropane (TMP)sodium phosphate, monobasic dehydrate, sodium chloride, ethylenediaminetetraacetic acid (EDTA), brilliant blue G, sodium hydroxide, sodium 8-Anilino-1-naphthalenesulfonate (ANS-Na), 6-FITC were bought from Macklin biochemical Co. Ltd. (Shanghai, China). All chemicals were of analytical grade.

2.2. Preparation of lipid oxidation products

MDA solution was prepared according to Wang et al. (2019) with some modifications. Briefly, TMP (1.1 mL) was added with distilled water (38.9 mL) and 5 M HCl (10 mL). The reaction was magnetically stirred at 50 °C for 1 h in the dark. The color of the solution changed from colorless to light yellow. The pH of the mixture was adjusted to 7.4 using 6 M NaOH after the temperature was lowered to room temperature. Dilute the solution appropriately and measure the absorbance at 267 nm with a UV–Vis spectrophotometer (UV1900i, Shimadzu, Kyoto, Japan). The concentration of MDA was determined by the specific absorbance coefficient (31500 M^{-1} cm^{-1}). The MDA solution was finally diluted in phosphate buffer B (25 mM, pH 7.0) containing 0.6 M NaCl to make 10 mM working solution. The HNE solution was diluted to a 10 mM solution in phosphate buffer B mentioned above.

2.3. Extraction of MP

The method for MP extraction was carried out in agreement with former reports (Shen et al., 2020). MP was stored at 4 °C and analyzed within 24 h. To determine the MP concentration, the volume of 20 μL MP solution was mixed with the 200 μL of Coomassie Brilliant Blue G-250 and the absorbance was measured at 595 nm.

2.3. In vitro oxidation of MP

The MP suspensions were adjusted to 1 mg mL^{-1} using the phosphate buffer B. The MP suspension without any addition was the control group, the 10 mM MDA and HNE solution were added into MP as treated groups, respectively. The solution was immediately equally divided into three portions for low temperature vacuum heating (LTVH). The temperature of this period was set as 50, 60, 70 °C respectively. The control groups were named C50, C60, and C70. The MP solutions treated with MDA were M50, M60, M70 while those treated with HNE were H50, H60, H70. After heating for 15 min, the resulting MP solutions were dialyzed against 20 mM phosphate buffer A (pH 7.0) comprising 100 mM NaCl and 1 mM EDTA for 10 h. At the end of dialysis, the suspension was centrifuged at 10,000 g for 15 min at 4 °C, and the supernatants were discarded. The precipitate was subsequently lysed with phosphate buffer B and adjusted the MP solution to 1 mg mL^{-1}.

2.4. Intrinsic fluorescence spectroscopy

The fluorescence emission spectrum was obtained using the methods reported by Chizoba Ekezie, Cheng, & Sun (2018) with some modifications. The fluorescence spectra were recorded at wavelengths ranging from 300 to 400 nm with the excitation wavelength at 285 nm. The excitation slit width was set at 5 nm and the emission slit width was the same.

2.5. Fourier transformation infrared (FTIR) spectroscopy

The infrared spectra of the MP samples were obtained using a Fourier transform infrared spectrometer (NICOLET IS5, Thermo Scientific, Germany). Samples were mixed with dry potassium bromide in a ratio of 1:100, ground, and pressed. The test was scanned in the range of 4000–400 cm^{-1} and performed in transmissive mode with 32 scans (Liu et al., 2021).

2.6. Surface hydrophobicity

MP samples (2 mL) was mixed with 20 μL of 1-anilino-8-naphthalenesulfonate (8 mM) and mixed vortex. After standing at room temperature for 3 min and being protected from light. The excitation and emission wavelengths were set at 390 and 470 nm, respectively (slit width 5 nm) (Guo, Jiang, True, & Xiong, 2021). The fluorescence spectrum for phosphate buffer B was subtracted from all sample spectra. The initial slope of the fluorescence intensity versus protein concentration (mg mL^{-1}) plot (calculated by linear regression analysis) was used as an index of surface hydrophobicity.

2.7. Fluorescence excitation-emission matrix (EEM) spectra

The three-fluorescence (3D) fluorescence emission spectra of MP were recorded using an RF-6000 fluorescence spectrophotometer (Shimadzu, Kyoto, Japan) as described by Lv et al. (2022) with modifications. The 3D map was collected with an excitation wavelength of 200–400 nm and an emission wavelength of 200–500 nm, with a 5 and 10 nm slit for excitation and emission, respectively.

2.8. Isothermal titration calorimetry (ITC)

The binding between lipid oxidation products (MDA and HNE) and MP was investigated using MicroCal PEAQ-ITC (Malvern Panalytical Limited, USA). MP was dissolved in a 6 M NaCl solution. 280 μL of MP solution was added to the sample cell and titrated with the MDA and HNE 19 times, respectively. The titrated samples were injected with a

time of 4 s per injection, 120 s between each injection, 0.4 μL per injection, and then 18 injections of the same 2 μL. The analyses were performed at 50, 60, and 70 °C, respectively.

2.9. Molecular docking

Molecular docking was performed to study the binding modes for the site of myosin with its ligands and obtain binding affinity (Xu et al., 2021, 2022). Molecular structure of MDA was obtained from the ZINC database (http://zinc.docking.org/substances/ZINC000005178380/). The 2D structures of HNE were obtained from the same website (http://zinc.docking.org/substances/ZINC000002020117/), which were then converted to PDB format via OpenBableGUI software. The crystal structure of myosin (PDB ID: 3QMA) was obtained from the RCSB Protein Data Bank (https://www.pdbus.org/structure/3QMA). The crystal structure was prepared into receptors by removing water and substrate and adding polar hydrogen atoms by AutoDock software. At the same time, AutoDock Vina was used to conduct protein–ligand molecular docking studies. A grid box covered the entire binding site was centered at coordinates of X: 42.75, Y: 46.5, and Z: 47.25. The position with the highest Vina docking score was chosen, and its visual analysis was performed by PyMoL software (https://www.pymol.org).

2.10. Statistical analysis

Data were expressed as means plus standard deviations for three independent experiments, each repeated four times. With the help of SPSS software (version 20.0), the significance between treatments was determined by using Multivariate Analysis of variance and least significant difference multiple comparison. The level for significance was defined as $P < 0.05$.

3. Results and discussion

3.1. Protein intrinsic fluorescence of the interaction between lipid oxidation products and MP

Intrinsic fluorescence quenching was used to study the potential interaction between MP and lipid oxidation products (MDA and HNE). There were two main forms of fluorescence quenching, one was protein–protein cross-linking resulting from protein oxidation and modification, and the other was the binding of covalent/non-covalent protein to lipid secondary oxidation ligands (such as MDA) (Zhang et al., 2022). Fig. 1 A showed the λ_{max} values of MP in each group, which was around 330 nm and the peak value was tryptophan (Try). An increase in the temperature led to a decrease in the fluorescence intensity of MP. It was consistent with Wan et al (2021). As the temperature increased, the degree of protein aggregation increased, causing an increase in steric hindrance, the fluorescence intensity decreased as well. The aggregation degree of protein increases with increasing the temperature, which results in the increasing of the steric hindrance and lower fluorescence intensity (Wan et al., 2021). The fluorescence intensity will be significantly reduced when the protein containing a tryptophan residue exposed into the hydrophilic environment, and the decrease in fluorescence intensity stated that the MP was in a partially unfolded or fully unfolded state (Cao & Xiong, 2015).

The response results of MDA and HNE were similar, with lower fluorescence intensity in higher temperatures. However, the fluorescence intensity decreased more after MDA treatment than HNE. It was reported that MDA can reduce protein fluorescence intensity due to the destruction of tryptophan residues, as well as the change of tryptophan microenvironment caused by the binding reaction of MDA to certain sites in the protein (Traverso et al., 2004). The lipid peroxidation product HNE reacted with proteins' histidine, cysteine, and lysine residues to form HNE-protein adducts (Schaur, 2003), which may be the reason for the less decrease in fluorescence of HNE.

3.2. Secondary structures of the interaction between lipid oxidation products and MP

Fig. 1B showed the secondary structure of the interaction between lipid oxidation products and MP subjected to the different heating temperatures. The secondary structure composition was determined by FTIR by measuring absorbance within the amide I region (1600–1701 cm^{-1}) (Shi et al., 2020), and the results were shown in Table 1. It was clear that the ratio of α-helix significantly decreased and β-sheet and random increased concomitantly with the temperature increasing ($P < 0.05$). It was conceptualized that intramolecular hydrogen bond networks played a critical role in the stability of α-helix, while heating weakened or even broke the hydrogen bond between the amino hydrogen and the carbonyl oxygen, thereby unwinding the α-helical

Table 1
Changes in secondary structure content of MP extracted from sturgeon fillets.

	α-helix/%	β-sheet/%	β-turn/%	Random/%
C50	13.60 ± 0.82^{a}	38.16 ± 0.10^{d}	34.78 ± 2.13^{a}	12.93 ± 0.71^{c}
C60	12.44 ± 0.27^{abc}	39.89 ± 0.64^{cd}	35.36 ± 0.50^{a}	12.28 ± 0.13^{c}
C70	11.71 ± 0.55^{bc}	41.90 ± 1.49^{bc}	32.77 ± 1.10^{ab}	17.60 ± 0.94^{a}
M50	12.83 ± 1.06^{ab}	39.63 ± 0.73^{d}	29.55 ± 2.52^{b}	15.98 ± 0.07^{ab}
M60	12.46 ± 0.67^{abc}	42.47 ± 1.77^{b}	35.07 ± 0.42^{a}	16.97 ± 1.35^{ab}
M70	11.69 ± 0.38^{bc}	45.49 ± 0.91^{a}	33.56 ± 1.81^{ab}	17.64 ± 0.07^{a}
H50	13.19 ± 0.33^{ab}	38.08 ± 0.15^{d}	32.93 ± 2.69^{ab}	15.28 ± 1.06^{b}
H60	11.81 ± 0.47^{bc}	39.98 ± 0.11^{cd}	34.32 ± 0.57^{a}	16.37 ± 0.69^{ab}
H70	10.98 ± 0.84^{c}	43.99 ± 0.38^{ab}	34.42 ± 1.92^{a}	17.09 ± 1.15^{ab}

Results are presented as the mean ± standard deviation. Different letters indicate significant difference ($P < 0.05$).
The heating temperature of MP was set as 50, 60, 70 °C respectively. The control groups were named C50, C60, and C70. The MP solutions treated with MDA were M50, M60, M70 while those treated with HNE were H50, H60, H70.

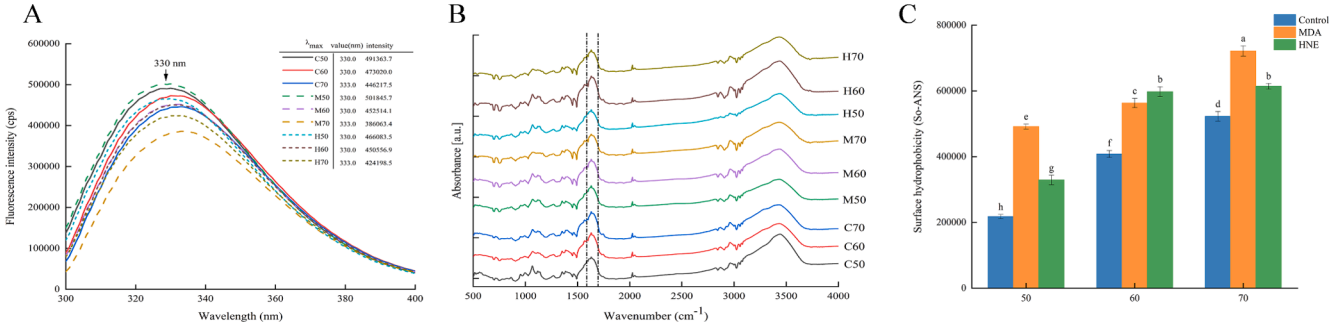

Fig. 1. Changes in intrinsic fluorescence (A) and secondary structure (B) of MP extracted from sturgeon fillets. The heating temperature of MP was set as 50, 60, 70 °C respectively. The control groups were named C50, C60, and C70. The MP solutions treated with MDA were M50, M60, M70 while those treated with HNE were H50, H60, H70.

structure of the protein (Yin, Zhou, Pereira, Zhang, & Zhang, 2020). Generally, the decline of the α-helix and the increase of the β-sheet usually indicated the unfolding of MP molecules with further aggregation and less structural order (Jiang et al., 2017; Zhang et al., 2022).

For the interaction of different lipid oxidation products and MP, the effect of MDA on MP was more obvious. The interaction between HNE and MP was beneficial to the unfolding of the α-helix segment in MP, which can expose HIS residues buried inside the molecule, such as HIS24 (Friend & Gurd, 1979), followed by further binding of HNE (Viana et al., 2020), making the MP helical structure slightly recycled, so compared with the control groups differences were not significant ($P > 0.05$). As for MDA, it reacted readily with ε-NH2 groups of MP and reported that MDA can modify proteins by reacting with 50–60% of ε-NH2 (Buttkus, 1967; Wang et al., 2017). Wang et al. (Wang et al., 2021) verified that MDA can reduce in α-helix and increase in the random coil of MP.

3.3. Tertiary structure of the interaction between lipid oxidation products and MP

ANS was a fluorescent probe with enhanced fluorescence after binding to a hydrophobic surface, which can be used to observe the conformational changes of proteins, mainly the exposure of hydrophobic regions (Fu et al., 2020). As depicted in Fig. 2, the effect of temperature on the surface hydrophobicity was very significant, the temperature increased, the surface hydrophobicity increased significantly ($P < 0.05$). The results were supported by Traore et al. (2012) who reported that increasing the heating temperature increased the surface hydrophobicity of pork MPs. After heating, part of non-polar amino acids was exposed to the hydrophobic clusters, leading to unfolding and rearrangement of protein molecules (Fu et al., 2019; Yarnpakdee, Benjakul, Visessanguan, & Kijroongrojana, 2009), increasing surface hydrophobicity, which was consistent with the result of Fourier transformation infrared spectroscopy. In addition, it was clear that the addition of MDA and HNE significantly increased the surface hydrophobicity ($P < 0.05$). Except that the surface hydrophobicity of the added MDA was lower than that of HNE in the 60 °C treatment group, the other two groups had the highest MDA. This indicated that due to the action of MDA, electrostatic interactions or hydrogen bonds between proteins are disrupted, resulting in the unfolding of proteins and exposing non-polar amino acids to the protein surface, thereby increasing the surface hydrophobicity (Wang et al., 2017; Wang et al., 2021).

Fluorescence excitation-emission matrix (EEM) spectra can simultaneously obtain and characterize the spectral peak information of different fluorophores of proteins, which contributed to the confidence

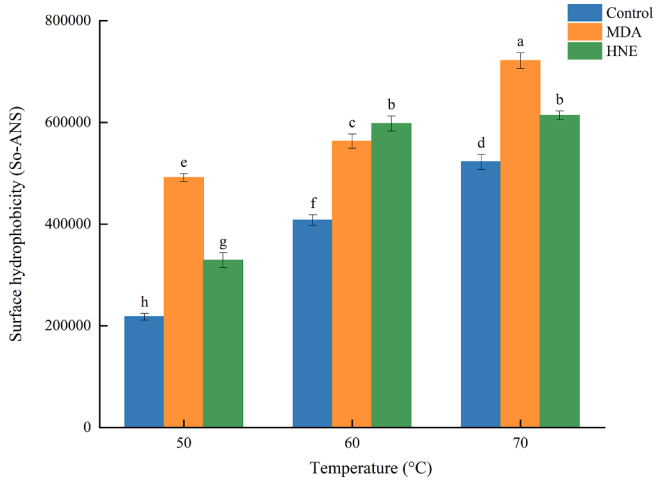

Fig. 2. Changes in surface hydrophobicity of MP extracted from sturgeon fillets.

of conformational studies (Fu et al., 2020). Fig. 3 showed the spectra of the interaction between lipid oxidation products and MP. Generally, Peak 1 (λex = 280.0 nm, λem = 330.0 nm) characterized the spectral properties of Trp and Tyr residues, and peak 2 (λex = 230.0 nm, λem = 330.0 nm) can represent the fluorescence spectral changes of the polypeptide backbone structure (Jin, Wang, Yang, Shan, & Feng, 2021; Lv et al., 2022). The fluorescence intensity in Fig. 3 showed decreasing trends as temperature increased, for both two peaks. Meanwhile, it can be observed that the peak 1 fluorescence intensity of MP decreased after adding MDA and HNE in heating conditions. Besides, the fluorescence intensity of peak 2 also decreased with the addition of MDA and HNE. The chromophores of peak1 were mainly tryptophan (Trp) and tyrosine (Tyr), which were usually located in the hydrophobic region of the protein. The changes in fluorescence intensity were usually due to swelling of proteins exposing them to a hydrophilic environment (Jin et al., 2021). The interaction of lipid oxidation products with MP altered the polarity of the microenvironment of Trp and Tyr residues, resulting in reduced MP polarity and enhanced hydrophobicity, and a tendency for the protein to fold (Lv et al., 2022), it was validated the conclusion of surface hydrophobicity and intrinsic fluorescence spectroscopy.

3.4. Affinity of lipid oxidation products to MP

It was reported that ITC was an important method to explain the mechanisms of interaction (Demers & Mittermaier, 2009). Dissociation constants (K_D), enthalpy change (ΔH), Gibbs free energy change (ΔG), and entropy change (ΔS) were crucial thermodynamic parameters for the investigation of interaction mechanism (Fu et al., 2020). A summary of the thermodynamic parameters from the ITC assay were presented in Table 2. The K_D value of MDA and MP was smaller than HNE ($P < 0.05$), suggesting that the binding capacity of MP with MDA was stronger than that with HNE. The negative values of ΔG indicated the feasible and spontaneous nature of reaction (Fu et al., 2020). Besides, according to the size of thermodynamic enthalpy and entropy change, the main types of ligand–protein binding can be obtained (Frazier, Papadopoulou, & Green, 2006). Through the symbols of some thermodynamic constants, the type of molecular bonds can be judged: When $\Delta H > 0$ and $\Delta S > 0$, the reaction was a typical hydrophobic interaction; when $\Delta H < 0$ and $\Delta S < 0$ represented van der Waals forces and/or hydrogen bonds; when $\Delta H \approx 0$ or less, $\Delta S > 0$ was an electrostatic interaction (Ross & Subramanian, 1981). It can be seen from Table 2 that both ΔH and ΔS of interaction lipid oxidation products and MP were negative, indicating that the major interaction forces in MP-MDA or MP-HNE complexation were hydrogen bonding and/or van der Waals forces. Besides, the increase in temperature made the K_D value decrease, indicating that increasing the temperature was beneficial to the reaction.

3.5. Molecular docking of the interaction between lipid oxidation products and MP

Molecular docking modeling was used to further validate the binding ability of lipid oxidation products and MP (Fig. 4). The binding energy of MP against MDA and HNE were −5.5 and −4.1 kcal/mol and indicated that the binding ability of MP to MDA was stronger than HNE. The results were consistent with the findings of the results of ITC. The HNE and MP complex was formed three conventional hydrogen bonds (O···H-X), in which the hydroxyl oxygen of HNE and the residues of LYS-67 formed two hydrogen bonds with the length of 3.0 Å and 3.2 Å, respectively (Fig. 4A). MDA was in close contact with HIS-78, LEU-71, and LEU-72, and formed six hydrogen bonds with the bond length of 3.5 Å, 3.0 Å, 2.8 Å, 2.1 Å, 1.8 Å and, 3.5 Å, respectively (Fig. 4B). The results showed that the lipid oxidation products interacted with MP through hydrogen bonds and further confirmation of the results of ITC. The weak interactions suggested that the binding between lipid oxidation products and MP was reversible. It was reported that amino acid residues in proteins provide a more favorable environment for the reaction of MDA (Esterbauer,

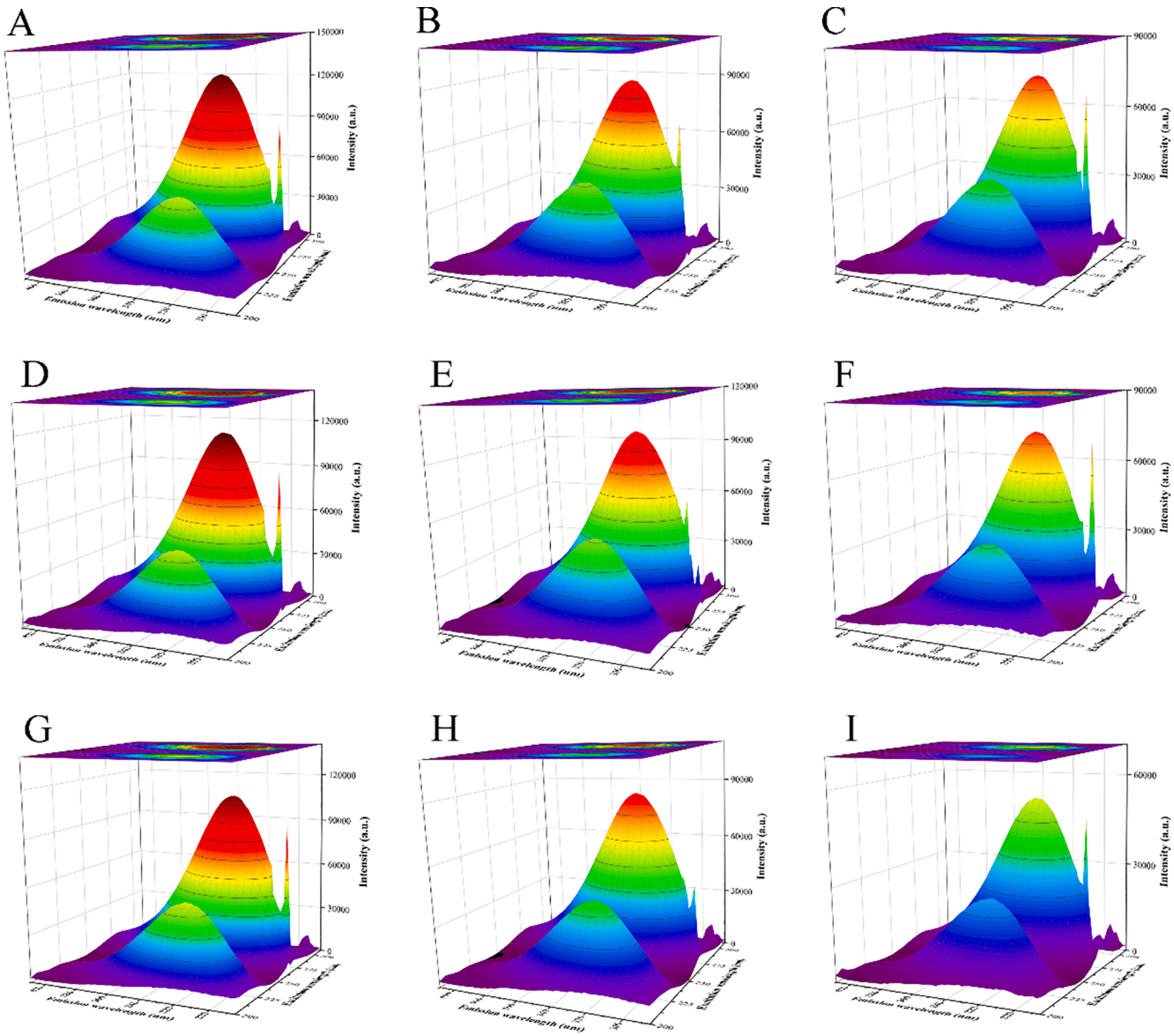

Fig. 3. Changes in Fluorescence excitation-emission matrix spectra of MP extracted from sturgeon fillets. A- C represented the control groups, D-F represented the MDA groups, G-I represented the HNE groups, from left to right, this were 50 °C, 60 °C, 70 °C.

Table 2
Changes in thermodynamic properties of MP extracted from sturgeon fillets.

	T (°C)	K_D (M, ×10-5)	ΔH (kcal/mol)	ΔG (kcal/mol)	-TΔS (kcal/mol)
MDA	50	12.1 ± 0.5^{c}	-1.5 ± 0.2^{c}	−29.8	28.9
	60	7.0 ± 1.1^{d}	-1.1 ± 0.3^{c}	−25.7	27.3
	70	2.9 ± 0.9^{e}	-0.8 ± 0.1^{d}	−25	23.8
HNE	50	36.3 ± 1.4^{a}	-3.3 ± 0.1^{a}	−78.9	261
	60	22.6 ± 0.3^{b}	-2.1 ± 0.2^{b}	−74.3	138
	70	10.5 ± 2.0^{c}	-1.6 ± 0.1^{c}	−76.6	123

Different letters indicate significant difference ($P < 0.05$).

Schaur, & Zollner, 1991). In general, His only reacted with the corresponding allyl group on the a-amino group, since MDA had an amino-imino-propene structure, it was easier to react with amino acids such as histidine and lysine. And the methyl-esters of His also reacted with MDA to enaminals of the general structure RNH-–CH=CH—CHO (Pietrzyk & Stodola, 1981).

4. Conclusion

In conclusion, the interactions of different lipid oxidation products (MDA and HNE) with MP in LTVH treatment and the corresponding effects on the structure at the molecular level were investigated using multispectroscopic and molecular docking. The addition of MDA and HNE altered the spatial structure of MP; however, this change was detrimental to the MP. And increasing the heating temperature can increase the damage degree of protein structure and make the fluorescence spectrum change more significant. The result of ITC showed that the lipid oxidation products interact spontaneously with MP and by hydrogen bonding, and molecular docking further confirmed this. However, the ability of MDA to bind to MP was stronger than that of HNE. The amino acid residues related to binding of MDA to MP were identified, and HIS-78, LEU-71, and LEU-72 was confirmed as the key amino acid residue. As for HNE, LYS-67 was the key amino acid residue. The results can provide a theoretical basis for the industrial application of modified proteins induced by lipid oxidation products. At present, we only study the interaction between lipid oxidation products and protein and the changes to the spatial structure of protein, but lack of research

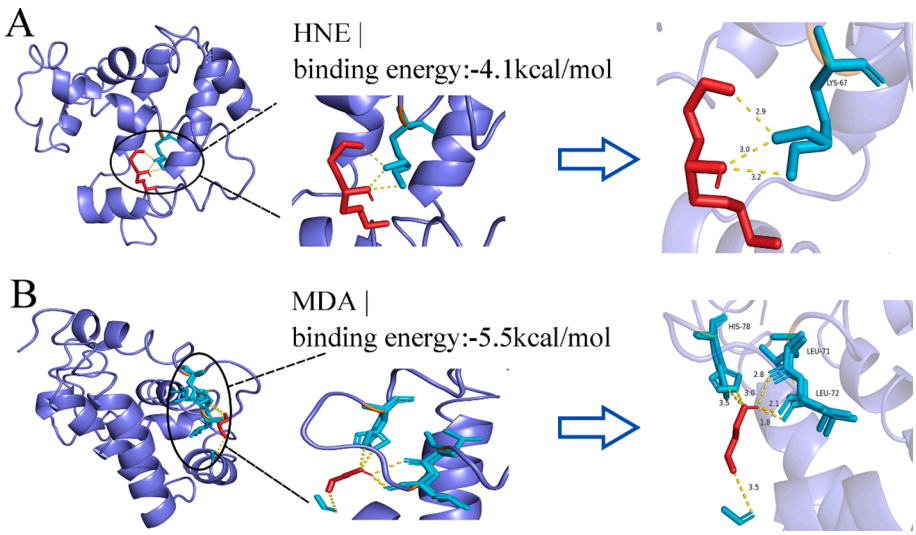

Fig. 4. The best docked conformations for the complex of MP with HNE (A) and MDA (B). The red stick structure was used to represent the lipid oxidation products, while the blue stick showed the MP. The dashed yellow line represented hydrogen-bonding.

and specific application of specific characteristics of protein. Further studies are needed to focus on the study of the emulsifying properties of the lipid oxidation products for protein and the loading capacity of the emulsion.

CRediT authorship contribution statement

Shi-ke Shen: Writing – original draft, Conceptualization. **Qian-yun Bu:** Methodology. **Wen-tao Yu:** Validation. **Yue-wen Chen:** Writing – review & editing, Validation. **Fei-jian Liu:** Writing – original draft, Conceptualization, Supervision. **Zhi-wen Ding:** Supervision. **Jun-long Mao:** Methodology.

Declaration of Competing Interest

The authors declare that they have no known competing financial interests or personal relationships that could have appeared to influence the work reported in this paper.

Acknowledgment

This work was financially supported by “National Key R&D Program of China (2018YFD0400600)”, “Foundation of Zhejiang Educational Committee (Y201942135)” and “Zhejiang Provincial Natural Science Foundation (LQ21C200004)”.

References

Buttkus, H. (1967). The reaction of myosin with malonaldehyde. *Journal of Food Science, 32*(4), 432–434. https://doi.org/10.1111/j.1365-2621.1967.tb09703.x

Cao, Y., & Xiong, Y. L. (2015). Chlorogenic acid-mediated gel formation of oxidatively stressed myofibrillar protein. *Food Chemistry, 180*, 235–243. https://doi.org/10.1016/j.foodchem.2015.02.036

Chizoba Ekezie, F.-G., Cheng, J.-H., & Sun, D.-W. (2018). Effects of mild oxidative and structural modifications induced by argon plasma on physicochemical properties of Actomyosin from King Prawn (Litopenaeus vannamei). *Journal of Agricultural and Food Chemistry, 66*(50), 13285–13294. https://doi.org/10.1021/acs.jafc.8b05178

Demers, J.-P., & Mittermaier, A. (2009). Binding mechanism of an SH3 domain studied by NMR and ITC. *Journal of the American Chemical Society, 131*(12), 4355–4367. https://doi.org/10.1021/ja808255d

Esterbauer, H., Schaur, R. J., & Zollner, H. (1991). Chemistry and biochemistry of 4-hydroxynonenal, malonaldehyde and related aldehydes. *Free Radical Biology and Medicine, 11*(1), 81–128. https://doi.org/10.1016/0891-5849(91)90192-6

Frazier, R. A., Papadopoulou, A., & Green, R. J. (2006). Isothermal titration calorimetry study of epicatechin binding to serum albumin. *Journal of Pharmaceutical and Biomedical Analysis, 41*(5), 1602–1605. https://doi.org/10.1016/j.jpba.2006.02.004

Fleuranceau-Morel, P., Barrier, L., Fauconneau, B., Piriou, A., & Huguet, F. (1999). Origin of 4-hydroxynonenal incubation-induced inhibition of dopamine transporter and Na+/K+ adenosine triphosphate in rat striatal synaptosomes. *Neuroscience Letters, 277*(2), 91–94. https://doi.org/10.1016/S0304-3940(99)00652-7

Friend, S. H., & Gurd, F. R. N. (1979). Electrostatic stabilization in myoglobin. The pH dependence of summed electrostatic contributions. *Biochemistry, 18*(21), 4612–4619. https://doi.org/10.1021/bi00588a023

Fu, Q., Liu, R., Wang, H., Hua, C., Song, S., Zhou, G., & Zhang, W. (2019). Effects of oxidation in vitro on structures and functions of Myofibrillar protein from beef muscles. *Journal of Agricultural and Food Chemistry, 67*(20), 5866–5873. https://doi.org/10.1021/acs.jafc.9b01239

Fu, X., Belwal, T., He, Y., Xu, Y., Li, L., & Luo, Z. (2020). Interaction and binding mechanism of cyanidin-3-O-glucoside to ovalbumin in varying pH conditions: A spectroscopic and molecular docking study. *Food Chemistry, 320*, Article 126616. https://doi.org/10.1016/j.foodchem.2020.126616

Guo, A., Jiang, J., True, A. D., & Xiong, Y. L. (2021). Myofibrillar protein cross-linking and gelling behavior modified by structurally relevant phenolic compounds. *Journal of Agricultural and Food Chemistry, 69*(4), 1308–1317. https://doi.org/10.1021/acs.jafc.0c04365

Jiang, W., He, Y., Xiong, S., Liu, Y., Yin, T., Hu, Y., & You, J. (2017). Effect of mild ozone oxidation on structural changes of silver carp (Hypophthalmichthys molitrix) myosin. *Food and Bioprocess Technology, 10*(2), 370–378. https://doi.org/10.1007/s11947-016-1828-5

Jin, S., Wang, M., Yang, H., Shan, A., & Feng, X. (2021). Dietary supplementation of resveratrol improved the oxidative stability and spatial conformation of myofibrillar protein in frozen-thawed duck breast meat. *Food Bioscience, 43*, Article 101261. https://doi.org/10.1016/j.fbio.2021.101261

Liu, C., Lv, N., Ren, G., Wu, R., Wang, B., Cao, Z., & Xie, H. (2021). Explore the interaction mechanism between zein and EGCG using multi-spectroscopy and molecular dynamics simulation methods. *Food Hydrocolloids, 120*, Article 106906. https://doi.org/10.1016/j.foodhyd.2021.106906

Liu, F.-J., Shen, S.-K., Chen, Y.-W., Dong, X.-P., Han, J.-R., Xie, H.-J., & Ding, Z.-W. (2022). Quantitative proteomics reveals the relationship between protein changes and off-flavor in Russian sturgeon (Acipenser gueldenstaedti) fillets treated with low temperature vacuum heating. *Food Chemistry, 370*, Article 131371. https://doi.org/10.1016/j.foodchem.2021.131371

Lv, Y., Liang, Q., Li, Y., Liu, X., Zhang, D., & Li, X. (2022). Study of the binding mechanism between hydroxytyrosol and bovine serum albumin using multispectral and molecular docking. *Food Hydrocolloids, 122*, Article 107072. https://doi.org/10.1016/j.foodhyd.2021.107072

Pietrzyk, D. J., & Stodola, J. (1981). Preparative liquid chromatography of 1:1 adducts derived from the reaction of malondialdehyde with amino acids. *Analytical Biochemistry, 117*(1), 245–249. https://doi.org/10.1016/0003-2697(81)90718-1

Ross, P. D., & Subramanian, S. (1981). Thermodynamics of protein association reactions: Forces contributing to stability. *Biochemistry, 20*(11), 3096–3102. https://doi.org/10.1021/bi00514a017

Schaur, R. J. (2003). Basic aspects of the biochemical reactivity of 4-hydroxynonenal. *Molecular Aspects of Medicine, 24*(4), 149–159. https://doi.org/10.1016/S0098-2997(03)00009-8

Shen, S.-K., Chen, Y.-W., Dong, X.-P., Liu, F.-J., Cai, W.-Q., Wei, J.-L., … Wang, Y.-R. (2020). Changes in food quality and microbial composition of Russian sturgeon (Acipenser gueldenstaedti) fillets treated with low temperature vacuum heating method during storage at 4°C. *Food Research International, 138*, Article 109665. https://doi.org/10.1016/j.foodres.2020.109665

Shen, S.-K., Chen, Y.-W., Dong, X.-P., Liu, F.-J., Cai, W.-Q., Wei, J.-L., … Lin, M.-M. (2020). The effect of different salt concentration and time combinations in physicochemical properties and microstructure of Russian sturgeon (Acipenser

gueldenstaedtii) fillets under vacuum impregnation. *Journal of Food Processing and Preservation, 44*(12), e14967. https://doi.org/10.1111/jfpp.14967

Shi, L., Xiong, G., Yin, T., Ding, A., Li, X., Wu, W., … Wang, L. (2020). Effects of ultra-high pressure treatment on the protein denaturation and water properties of red swamp crayfish (Procambarus clarkia). *LWT-Food Science and Technology, 133*, Article 110124. https://doi.org/10.1016/j.lwt.2020.110124

Traore, S., Aubry, L., Gatellier, P., Przybylski, W., Jaworska, D., Kajak-Siemaszko, K., & Santé-Lhoutellier, V. (2012). Effect of heat treatment on protein oxidation in pig meat. *Meat Science, 91*(1), 14–21. https://doi.org/10.1016/j.meatsci.2011.11.037

Traverso, N., Menini, S., Maineri, E. P., Patriarca, S., Odetti, P., Cottalasso, D., … Pronzato, M. A. (2004). Malondialdehyde, a lipoperoxidation-derived aldehyde, can bring about secondary oxidative damage to proteins. *The Journals of Gerontology Series A: Biological Sciences and Medical Sciences, 59*(9), B890–B895.

Viana, F. M., Wang, Y., Li, S., Conte-Junior, C. A., Chen, J., Zhu, H., & Suman, S. P. (2020). Thermal instability induced by 4-hydroxy-2-nonenal in beef myoglobin. *Meat and Muscle Biology, 4*(1).

Wan, H., Li, H., Lei, Y., Xie, P., Zhang, S., Wang, H., … Sun, B. (2021). Influence of stewing conditions on tenderness and protein structure in beef. *Journal of Food Processing and Preservation, 45*(3), e15208.

Wang, J., Zhao, M., Qiu, C., & Sun, W. (2018). Effect of malondialdehyde modification on the binding of aroma compounds to soy protein isolates. *Food Research International, 105*, 150–158. https://doi.org/10.1016/j.foodres.2017.11.001

Wang, L., Zhang, M., Fang, Z., & Bhandari, B. (2017). Gelation properties of myofibrillar protein under malondialdehyde-induced oxidative stress. *Journal of the Science of Food and Agriculture, 97*(1), 50–57. https://doi.org/10.1002/jsfa.7680

Wang, Z., He, Z., Emara, A. M., Gan, X., & Li, H. (2019). Effects of malondialdehyde as a byproduct of lipid oxidation on protein oxidation in rabbit meat. *Food Chemistry, 288*, 405–412. https://doi.org/10.1016/j.foodchem.2019.02.126

Wang, Z., He, Z., Zhang, D., Chen, X., & Li, H. (2021). The effect of linalool, limonene and sabinene on the thermal stability and structure of rabbit meat myofibrillar protein under malondialdehyde-induced oxidative stress. *LWT-Food Science and Technology, 148*, Article 111707. https://doi.org/10.1016/j.lwt.2021.111707

Xu, L., Zheng, Y., Zhou, C., Pan, D., Geng, F., Cao, J., & Xia, Q. (2021). Kinetic response of conformational variation of duck liver globular protein to ultrasonic stimulation and its impact on the binding behavior of n-alkenals. *LWT-Food Science and Technology, 150*, Article 111890. https://doi.org/10.1016/j.lwt.2021.111890

Xu, L., Zheng, Y., Zhou, C., Pan, D., Geng, F., Cao, J., & Xia, Q. (2022). A structural explanation for enhanced binding behaviors between β-lactoglobulin and alkene-aldehydes upon heat- and ultrasonication-induced protein unfolding. *Food Hydrocolloids, 130*, Article 107682. https://doi.org/10.1016/j.foodhyd.2022.107682

Yarnpakdee, S., Benjakul, S., Visessanguan, W., & Kijroongrojana, K. (2009). Thermal properties and heat-induced aggregation of natural actomyosin extracted from goatfish (Mulloidichthys martinicus) muscle as influenced by iced storage. *Food Hydrocolloids, 23*(7), 1779–1784. https://doi.org/10.1016/j.foodhyd.2009.03.006

Yin, Y., Zhou, L., Pereira, J., Zhang, J., & Zhang, W. (2020). Insights into digestibility and peptide profiling of beef muscle proteins with different cooking methods. *Journal of Agricultural and Food Chemistry, 68*(48), 14243–14251. https://doi.org/10.1021/acs.jafc.0c04054

Zhang, M., Li, C., Zhang, Y., Pan, J., Huang, S., Lichao, H., & Jin, G. (2022). Impact of salt content and hydrogen peroxide-induced oxidative stress on protein oxidation, conformational/morphological changes, and micro-rheological properties of porcine myofibrillar proteins. *Food Chemistry, 370*, Article 131074. https://doi.org/10.1016/j.foodchem.2021.131074

Zhang, W., Xiao, S., & Ahn, D. U. (2013). Protein oxidation: basic principles and implications for meat quality. *Critical Reviews in Food Science and Nutrition, 53*(11), 1191–1201. https://doi.org/10.1080/10408398.2011.577540